Nota

RILL EROSION ON AN OXISOL INFLUENCED BY A THIN COMPACTED LAYER[1]

Edivaldo Lopes Thomaz[2]

SUMMARY

The presence of compacted layers in soils can induce subprocesses (e.g., discontinuity of water flow) and induces soil erosion and rill development. This study assesses how rill erosion in Oxisols is affected by a plow pan. The study shows that changes in hydraulic properties occur when the topsoil is eroded because the compacted layer lies close below the surface. The hydraulic properties that induce sediment transport and rill formation (i.e., hydraulic thresholds at which these processes occur) are not the same. Because of the resistance of the compacted layer, the hydraulic conditions leading to rill incision on the soil surface differed from the conditions inducing rill deepening. The Reynolds number was the best hydraulic predictor for both processes. The formed rills were shallow and could easily be removed by tillage between crops. However, during rill development, large amounts of soil and contaminants could also be transferred.

Index terms: conventional tillage, plow-pan, hydropedology, surface runof, rill erosion.

RESUMO: *EROSÃO EM RAVINA EM UM LATOSSOLO INFLUENCIADO POR UMA CAMADA COMPACTADA RASA*

A presença de uma camada compactada no solo pode induzir a subprocessos como a descontinuidade hidráulica e impor outros limiares para a erosão dele e o desenvolvimento de ravina. Neste estudo foi avaliado como a erosão em ravina em um Latossolo é influenciada por um pé-de-grade. No estudo ficou demonstrado que ocorre mudança nas variáveis hidráulicas quando o topo do solo é erodido e a camada compactada fica próxima da superfície. Além disso, as variáveis para o transporte de sedimento e as para a incisão da ravina não foram as mesmas. Por causa da resistência da camada, as condições hidráulicas para a incisão da ravina no topo do solo não foram suficientes para causar o aprofundamento dela. O Número

---

[1] Received for publication on November 21, 2012 and approved on June 24, 2013. Study funded by the Brazilian Council for Scientific and Technological Development (CNPq) (Edital Universal MCT/CNPq 14/2009) (Protocol 473809/2009-5).

[2] Adjunct Professor, Geography Departament, South-Central State University - UNICENTRO. Street Simeão Camargo Varela de Sá, 3. Mail Box 3010. Postal Code 85.040-430 Guarapuava (PR), Brazil. E-mail: edivaldo.thomaz@pq.cnpq.br

de Reynolds foi a variável hidráulica que melhor explicou a incisão da ravina e o transporte de sedimento. Os sulcos formados foram superficiais, podendo ser facilmente removidos de uma cultura para outra durante o processo de plantio. No entanto, durante o desenvolvimento da ravina, grandes quantidades de sedimentos e contaminantes podem ser transferidas.

Termos de indexação: cultivo convencional, pé-de-grade, hidropedologia, escoamento superficial, ravina.

INTRODUCTION

This study shows how a compacted layer (plow layer) influenced rill development in clay soil (Oxisols), using a plot-scale experiment. It also shows that the hydraulic variables leading to rill formation (i.e., threshold) were not the same as the variables associated with sediment transport. The Reynolds number was the best hydraulic predictor for both processes. Additionally, because of the differential resistance of the compacted layer, the hydraulic conditions for rill incision on the soil surface differed from the conditions required for increasing the depth of the rill.

Although all farming systems are subject to compaction, plow pans typically develop in the conventional tillage system because of the use of implements that disturb the topsoil and compacted subsurface layers (Hamza & Anderson, 2005). This system, therefore, frequently leads to effects such as increased compaction, reduced macroporosity and hydraulic conductivity, and a decrease in infiltration (Morgan, 2005; Hemmat et al., 2007; Blanco & Lal, 2010). A compacted layer has physical characteristics (e.g., resistance and permeability) that differ from the layers above and below. As a result, the plow layer leads to anisotropy between the soil layers (e.g., hydraulic discontinuity).

Similarly, the farming systems induce soil erosion and degradation. In agricultural soils, the following types of soil erosion have been investigated: interril erosion, rill erosion, tillage erosion, bioerosion, and harvest erosion (Evans, 1998; Bryan, 2000; Ruysschaert et al., 2004; Stroosnijder, 2005; van Oost et al., 2006; Knapen et al., 2007).

Soil erosion by water occurs in three phases, which include the detachment, transport, and deposition of soil particles. The control of soil erosion by water must take the hillslope and soil characteristics into account, and scales which are related to flow pathways in agricultural systems (Auzet et al., 2002; Stroosnijder, 2005; Boix-Fayos et al., 2006; Thomaz & Vestena, 2012).

Most soil erosion studies have primarily focused on topsoil resistance to concentrated flow erosion (Bryan, 2000; Greene & Hairsine, 2004; Knapen et al., 2007; Smith et al., 2007), and few reports have discussed the effects of erosion on soil with a compacted layer (Bertolino et al., 2010; Rockwell, 2011).

The presence of a compacted layer can induce subprocesses and other conditions that can cause soil erosion and rill development. The aim of this study was to assess the erosion of soil affected by a thin compacted layer. This form of erosion is common in tropical soils under conventional tillage, which is widely used throughout the world (Lal, 2007; Huggins & Reganold, 2008).

MATERIAL AND METHODS

The experiment was conducted in Guarapuava in the State of Paraná, Brazil (1018 m asl; coordinates 25º 22' 25 S, 51º 29' 42 W; Figure 1). The study was developed in clay-textured Oxisols (USDA soil taxonomy). The mean slope of the experimental area was 0.07 m m^{-1}. The data on granulometry, chemical properties, organic carbon content, and grain size are shown in table 1.

A plot-scale experiment was performed to evaluate the influence of a thin compacted soil layer on rill development. The soil was prepared using three harrowing operations. Two harrowing operations with a disk harrow (heavy hoe) were preformed perpendicular to the slope, reaching a depth of ~0.20 m. One harrowing operation was performed with a leveling harrow at a depth ~0.15 m. After leveling, the soil was left fallow for approximately one year. The soil was then harrowed manually, reaching a depth of 0.05 m, to remove weeds and smoothen the surface roughness. The plots were bordered by a 5 × 1 m sheet metal, installed along the slope direction. The plot sizes used in this study were within the limits reported for field investigations in the literature (Knapen et al., 2007). The simulations were applied to bare soil that had been smoothened before each simulation. At the lower end of the plot, a trough was installed to measure the runoff and sediment carried away during the simulation. Throughout the test, runoff and sediment were collected at 1-min intervals. The collected material was taken to the laboratory for drying and weighing.

A sprinkler, consisting of a framework of iron pipes (¾"), a nozzle installed at a height of 5 m, and a 2.5-HP gasoline water pump were used to supply water. The diameter of the water droplets varied from 0.35 to 6.35 mm, with a median of 2.40 mm. The device produced rain with 90 % of the kinetic energy of natural rainfall and at a similar intensity (Merz & Bryan, 1993).

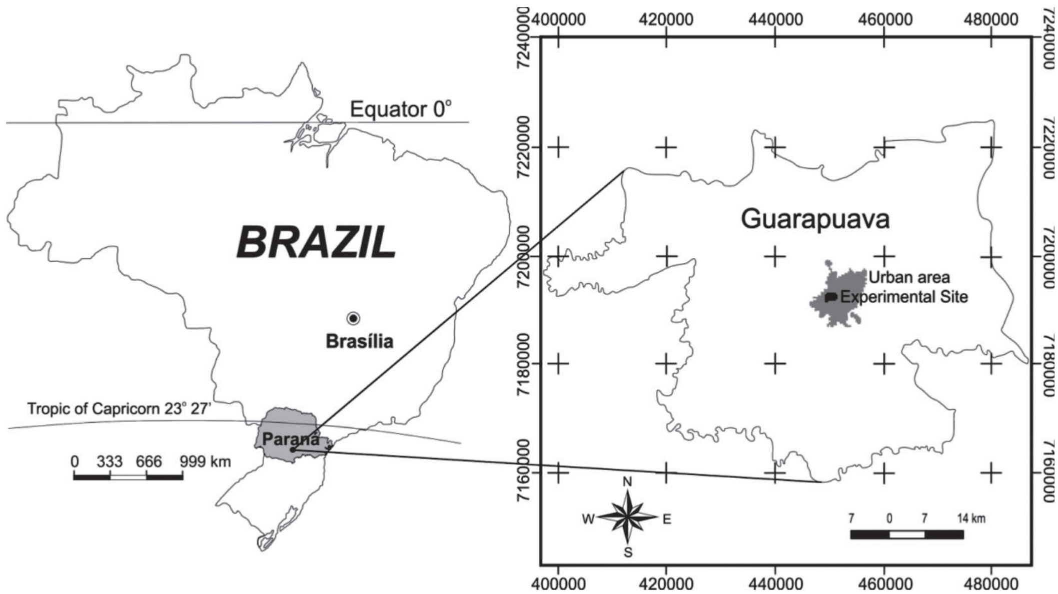

Figure 1. Location of the study area and experimental site (ES).

Table 1. Soil characteristics

Depth	Clay	Silt	Sand	OC[(1)]	pH ($CaCl_2$)[(2)]
cm	kg kg^{-1}			g dm^{-3}	
0-20	0.750	0.150	0.100	17.4	5.5
20-40	0.760	0.130	0.110		
40-60	0.770	0.130	0.100		
Grain size[(3)]	Dry sieve		Wet sieve		
mm	%				
4.0	11.0 ± 2.9		7.9 ± 2.7		
2.0	17.8 ± 1.7		20.7 ± 3.6		
1.0	20.1 ± 0.9		19.6 ± 1.3		
0.5	15.7 ± 0.7		19.0 ± 1.3		
0.250	14.7 ± 1.0		14.3 ± 1.5		
0.125	11.0 ± 1.1		18.5 ± 3.7		
<0.125	9.7 ± 1.3		No recorded		
Total	100.0		100.0		

[(1)] OC: organic carbono (Method Walkley-Black); [(2)] $CaCl_2$ 0.01 mol L^{-1}; [(3)] n = 5.

The current experiment was designed to mimic natural phenomena and control the environmental variables, which are crucial for generalized conclusions. Nonetheless, the control of variables in a field experiment can be rather difficult (Church, 2011). The experimental conditions should be as realistic as possible, especially with regard to the experimental variables (Dunkerley, 2008). There is a lack of correspondence between natural and simulated rain events. The rainfall intensity used in the experiments, for instance, was limited by the capacity of the simulator (Dunkerley, 2008).

To make the rainfall simulation more realistic, a total of 71 natural rains in a typical year (1920 mm) in the subtropical region of Guarapuava were analyzed for volume (mm), intensity (mm h), and duration (h or min) (Thomaz & Vestena, 2012).

The average rainfall event was 21.9 ± 20.2 mm, at an intensity of 6.6 ± 7.7 mm h^{-1}, lasting on average 4.3 ± 3.8 h. During this period, two important rainfall events occurred. The first event registered a volume of 51.6 mm with a peak intensity of 34.2 mm h^{-1} and lasted 90 min. The volume of the second precipitation event was 23.8 mm with a peak intensity of 47.4 mm h^{-1} and lasted 30 min. Thus, experimental rain simulated realistic and typical events for the region. Furthermore, the rain intensity in this study was more realistic than in most studies in the literature, which used simulated rainfall in field experiments (Dunkerley, 2008).

Rain was simulated at a rate of 31.1 ± 5.9 mm h^{-1} for 60 min to homogenize the soil surface. Precipitation was measured with 13 manual rain gauges distributed at the edges of the plot. Variations in rainfall during the experiment were caused by wind disturbance and pump operations. However, the rainfall volume and intensity were measured at the end of the experiment. After this phase of simulation, an extra flow (run-on) of 15.1 ± 1.0 L min^{-1} was applied for 30 min. The flow was released in the upper plot. During the run-on, the rain remained constant for 30 min. The flow was controlled by an electric pump (1/3 HP), which minimized variation (Table 2).

While it is difficult to control the variations of experimental rain (i.e., volume, intensity, and duration), it is even harder to adjust an extra flow (run-on). An extensive literature review revealed a minimum run-on value of 24.0 ± 40.8 L min^{-1}, and volumes of up to 107.7 ± 204.8 have been utilized (Knapen et al., 2007). In most run-on experiments,

Table 2. Rainfall simulation characteristics: rainfall intensity (RI), run-on, water temperature (WT) and electrical conductivity (EC)

RUN	RI(1)	Run-on	WT	EC
	mm h^{-1}	L min^{-1}	°C	µS
1	38.5	16.7	21.7	72.5
2	29.1	14.0	23.7	72.5
3	35.2	15.0	21.3	nr(2)
4	29.3	15.0	21.5	73.6
5	23.3	15.0	18.5	72.1
Average	31.1	15.1	21.4	72.7
SD(1)	5.9	1.0	1.9	0.6

(1)SD: standard deviation; (2)nr: no recorded.

no explanations were given for the use of certain flow rates. In a previous study by Thomaz & Vestena (2012), the authors showed that during one year, even after high-intensity and long-duration rainfalls, no rill was formed in the Oxisol. Therefore, a reasonable amount of extra flow was used to produce the effect of rill development. The extra flow used in this study was consistent with that reported in the literature, particularly in studies with a smaller discharge (Knapen et al., 2007).

The flow velocity and depth were measured throughout the run-on duration in the upper plot sector. During RUN 1 and RUN 2, there was no clear rill development. The flow was considered to be concentrated (i.e., surface runoff). During RUN 3, the flow was predominantly a rill flow. In this case, ~5 min of run-on was sufficient to induce rill incision. Thus, measurements of the flow velocity and depth were measured in the rill flow.

The flow velocity and depth were both measured at 5-min intervals, and the average values were determined after three replications. The flow velocity and depth were measured in the upper plot (1.5 m), the middle plot (3.0 m), and the lower plot near the trough (4.5 m). Thus, the flow velocity and depth were reported as the average of the three sectors (i.e., the whole plot). Therefore, each parameter was measured in at least nine replications to obtain the final average.

The flow depth was measured with a thin ruler. Dye tracing (i.e., blue methylene) was used to measure the runoff velocity. The flow velocity was determined by measuring the time it took for the flow to carry a dye plume from one point to another (distance 50 cm) (Farenhorst & Bryan, 1995). The flow velocity was measured at a shorter distance (Fox & Bryan, 1999). When measuring the flow velocity at a distance >1 m, the dye tracing concentration was reduced making it difficult to visualize the dye plume. The flow velocity rate was corrected by multiplying the velocity by the conversion factor for the surface velocity (0.67; Bryan, 1990).

The hydraulic flow conditions related to rill erosion and sediment transport were assessed using the following equations (see below). Additionally, the water temperature was measured during the experiment to correct for the differences in kinematic viscosity and water density (Table 2) (Julien, 1998).

$$Re = VR/v$$

where Re is the Reynolds number, V is the flow velocity (m s^{-1}), R is the hydraulic radius (m), and v is the fluid viscosity (m^2 s^{-1}).

$$Fr = V/(gR)^{0.5}$$

where Fr is the Froude number, V is the flow velocity (m s^{-1}), and g is the acceleration due to gravity (m s^{-2}).

$$ff = 8gRS/V^2$$

where ff is the Darcy-Weisbach friction factor, g is the acceleration due to gravity (m s^{-2}), R is the hydraulic radius (m), S is the slope (m m^{-1}), and V is the flow velocity (m s^{-1}).

$$\tau = \rho gRS$$

where τ is the shear stress (Pa), ρ the water density (kg m^{-3}), g the acceleration due to gravity (m s^{-2}), R the hydraulic radius (m), and S is the slope (m m^{-1}).

$$\omega = \rho gqS$$

where ω is the stream power (W m^{-2}), ρ the water density (kg m^{-3}), g the acceleration due to gravity (m s^{-2}), q the discharge (m^3 s^{-1}), and S is the slope (m m^{-1}).

$$u^* = \sqrt{gRS}$$

where u^* is the shear velocity (m s^{-1}), R the hydraulic radius (m), and S the slope (m m^{-1}).

$$VS = \text{unit stream power}$$

where V is the flow velocity (m s^{-1}) and S the slope (m m^{-1}).

The shear strength of the topsoil was measured by a Torvane pocket penetrometer. Measurements were only taken from the third experiment (RUN 3) because rill incision occurred during this experiment (i.e., marks of flow incision). The soil shear strength (i.e., penetration resistance) and depth were measured using an impact penetrometer (IAA/Planalsucar-STOLF) (Stolf, 1991). The measurement was performed in different sectors of the plot. Both measurements (i.e., with the torvane and impact penetrometer) were performed after the simulation experiment on wet soil (~40 % soil moisture by mass).

The data were analyzed using a simple regression analysis, and the average, standard deviation, and coefficient of variation. A Student's t-test was applied at the level of 5 % for comparisons of soil strength as measured by the pocket torvane on the interril and rill surfaces.

RESULTS

The sediment concentration (SC) increased sevenfold, and the runoff increased twofold from RUN 1 to RUN 5. In general, the surface runoff was more stable throughout the experiments. However, the SC was relatively unstable throughout the experiments (Figure 2).

In RUN 1, SC was lower at the beginning of the experiment. While the surface runoff increased by only 3 %, SC increased ninefold after 13 min. In RUN 2, SC was higher in the beginning (13 min of simulation) but SC decreased by ~40 % thereafter.

RUN 3 showed an SC greater than the surface runoff at the onset of the experiment. Subsequently, there was a reduction in the sediment that increased again afterwards. However, this was followed by a gradual reduction in sediment production. Also, the increased sediment peaks were also followed by a reduction in runoff (Figure 2).

In RUN 4, the runoff was primarily stable and only slightly reduced at the peaks of sediment production. Sediment production was variable (peaks) throughout the simulation. During the peaks, the pulse runoff reduction ranged from 5 to 13.6 %. the sediment production pattern in RUN 5 was similar to RUN 4, with several peaks and a decrease in SC. The runoff also decreased by up to 14 % during the sediment peaks (Figure 2).

The data for the hydraulic conditions in each experiment are shown in table 3. The greatest variability was recorded for the SC and Darcy-Weisbach friction factor. The other variables (e.g., flow depth, flow velocity, and shear stress) varied only moderately and slightly (e.g., discharge, stream power, and shear velocity). Except for the Darcy-Weisbach friction factor, the average values for the hydraulic variables increased as the experiment progressed, while the Darcy-Weisbach friction factor decreased.

The values of the hydraulic variables in RUN 1 and RUN 2 were lower than those of RUN 4 and RUN 5, except for the Darcy-Weisbach friction factor. The hydraulic conditions in RUN 3 were transitional, compared to the previous experiments. Although the flow was concentrated (i.e., the rill flow) in RUN 4 and RUN 5, the flow depth was shallow. In all experiments, the hydraulic flow conditions were turbulent (*Re* > 2000) and subcritical (*Fr* <1.0).

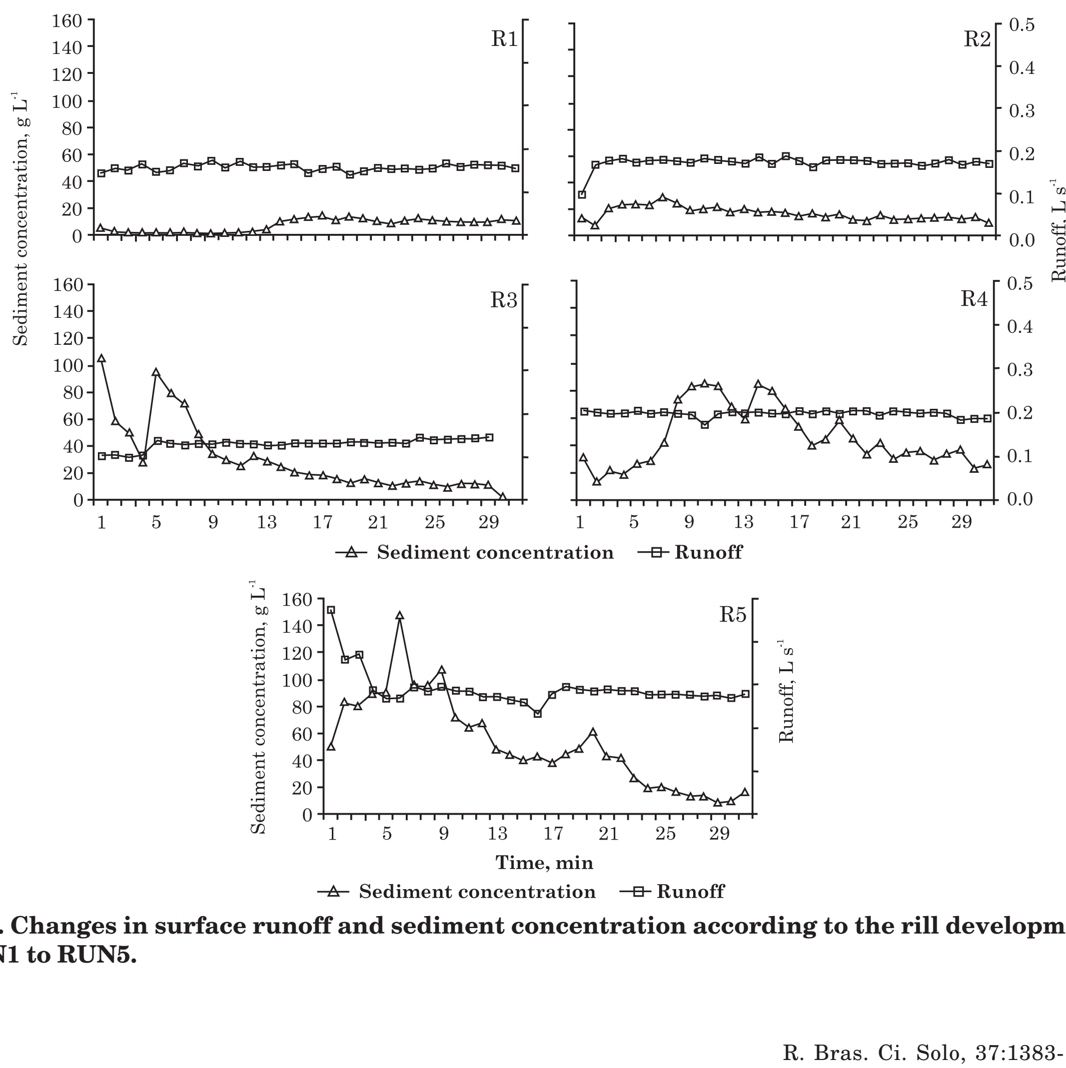

Figure 2. Changes in surface runoff and sediment concentration according to the rill development, from RUN1 to RUN5.

Table 3. Hydraulic variables of the surface runoff

Hydraulic variable	RUN 1	RUN 2	RUN 3	RUN 4	RUN 5
			Average (CV%)		
Discharge (Q) (L s^{-1})	0.157 (3.5)	0.172 (4.1)	0.130 (8.8)	0.198 (1.9)	0.290 (10.5)
Sediment concentration (SC) (g L^{-1})	7.34 (59.3)	16.71 (24.1)	31.13 (76.0)	47.17 (42.3)	53.75 (61.5)
Flow velocity (V) (m s^{-1})	0.084 (31.0)	0.09 (10.5)	0.094 (24.9)	0.129 (19.6)	0.151 (17.1)
Flow depth (R) (m)	0.01 (23.3)	0.007 (17.1)	0.013 (7.2)	0.014 (24.0)	0.014 (6.7)
Slope (S) (m m^{-1})	0.085	0.085	0.085	0.085	0.085
Reynolds number (Re)	3,453 (29.0)	2,800 (19.7)	4,988 (50.1)	7,906 (34.4)	8,522 (13.9)
Froude number (Fr)	0.281 (39.9)	0.350 (13.6)	0.269 (26.5)	0.348 (17.5)	0.423(10.7)
Darcy-Weisbach friction factor (ff)	15.35 (77.5)	6.23 (27.8)	11.43 (50.1)	6.74 (48.2)	4.05 (21.7)
Shear stress (τ) (Pa)	8.4 (23.3)	5.78 (17.1)	10.58 (7.2)	11.7 (24.0)	11.18 (13.2)
Stream power (ω) (w m^{-2})	26.17 (3.5)	28.56 (1.3)	21.6 (8.8)	32.98 (1.9)	48.27 (10.5)
Shear velocity (u*) (m s^{-1})	0.091 (11.9)	0.076 (8.8)	0.103 (3.6)	0.107 (12.3)	0.104 (10.6)
Unit stream power (VS) (m s^{-1})	0.007 (31.0)	0.008 (10.5)	0.008 (24.9)	0.011 (19.6)	0.013 (17.1)

n = 30 (for most variables)

The hydraulic variables were modeled according to the sediment transport (Figure 3). Additionally, all equations were modeled according to the average hydraulic conditions of the experiment. The best hydraulic variable predictions for sediment transport were as follows: 1) Reynolds number, 2) flow velocity, and 3) unit stream power.

Other hydraulic variables (e.g., shear stress and shear velocity) were not particularly reliable in predicting sediment transport; nonetheless, they were able to differentiate changes in the hydraulic conditions between the interrill flow (RUN1 and RUN 2) and rill flow (RUN 4 and RUN 5) (Figure 4). However, the Reynolds number clearly indicated hydraulic changes in each experiment, including the transitional condition (RUN 3), where the flow began to change from surface runoff to a well-defined rill flow (RUN 3 and RUN 4).

The soil strength was 38 % lower in the surface layer (0-10 cm), compared to the soil strength measured at the rill bottom (Figure 5a). The soil strength in the 10-15 cm depth range was 130 % higher than that recorded in the surface layer (0–10 cm) (Figure 5b). The greatest soil strength was recorded in the 20-25 cm depth range. In this layer, the soil strength was twice as high as in the surface layer (0-10 cm). Below a depth of 30 cm, the soil strength was homogeneous.

DISCUSSION

A change in hydraulic variables occurs when the topsoil is eroded and the compacted layer comes to lie closer beneath the surface. This removal of the loose soil surface layer causes the compacted layer to appear, affecting the topsoil strength and its hydraulic mechanisms.

In RUN 1 and RUN 2, SC and runoff were lower because there was no rill formation. At this stage, the topsoil was preserved and resistant to the hydraulic forces of surface runoff. Additionally, sediment exhaustion was not observed during the experiment. This process would indicate that the system was transport limited.

In RUN3 to RUN5, the topsoil had been partially depleted, and the compacted layer was closer to the surface. Thus, even without rill deepening, the rill incision increased the SC more than threefold when compared to the erosion caused by surface runoff.

Furthermore, in this simulation (RUN3 to RUN5), sediment exhaustion was observed, which indicated that the system was detach-limited. After rill incision, the flow was channeled along the rill (i.e., rill flow). The compacted layer prevented rill deepening and sediment detachment (Figure 6). However, the values of the hydraulic flow variables were high, especially towards the end of the experiment. At that time, the same hydraulic conditions (energy) that eroded the top soil were not able to not erode the compacted layer.

The hydraulic variables indicated that the threshold for rill incision differed from the variables related to the sediment transport. Rill incision occurs at a Reynolds number of ≥5000, a shear stress of ~11 (*Pa*), and shear velocity of ≥0.1 m s^{-1}. The following hydraulic variables were related to sediment production: Reynolds number, flow velocity, and unit stream power. All variables were related to flow velocity, and Re was a good predictor for both rill incision and sediment transport.

Clay soils are known to be more resistant to soil erosion than other soil types (Knapen et al., 2007). Consequently, the thresholds for rill incision and sediment transport are high when compared to soils

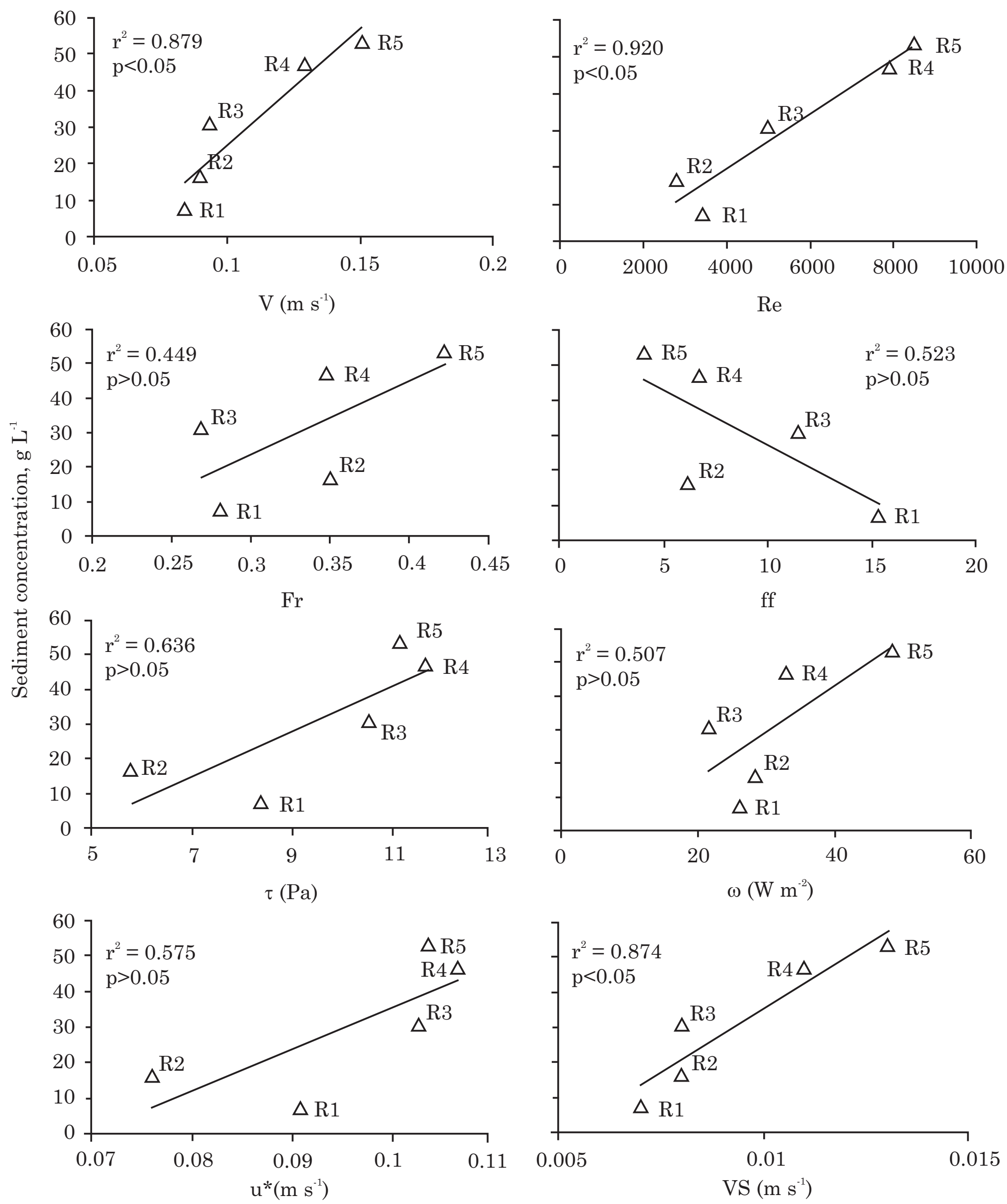

Figure 3. Hydraulic flow conditions and sediment transport.

with more silt and sand contents. Furthermore, there is no consensus concerning the best predictors for rill incision, sediment detachment, or sediment transport (Bryan, 2000; Govers et al., 2007; Knapen et al., 2007). Therefore, a straightforward comparison of the results of this study with those described in the literature is difficult, particularly because of the context of the experiment (e.g., experimental setup and variability). Moreover, most studies focused on topsoil strength, and little attention was paid to the compacted layer. However, laboratory experiments have provided some insight into the effect of the compacted layer on soil erosion, particularly on agricultural lands (Rockwell, 2011).

Conventional tillage requires the use of various mechanical implements. Therefore, in the current agricultural system, the formation of compacted subsurface layers is rather common (Figure 6a). The depth of the compacted layer beneath the soil surface varies widely, from 10 to 60 cm (Hamza & Anderson, 2005).

Agricultural implements (e.g., cultivators, harrows, harrow discs, rippers, and moldboards) operate at different depths. Generally, the tillage depth of the instruments varied from <5 cm to ~40 cm (van Oost et al., 2006; Bertolino et al., 2010). The plowing depth can reach down to 50 cm in some cases (Blanco & Lal, 2010). Thus, each implement may have created a compacted layer with specific physical characteristics. As a result, the hydraulic flow conditions for rill formation might also vary.

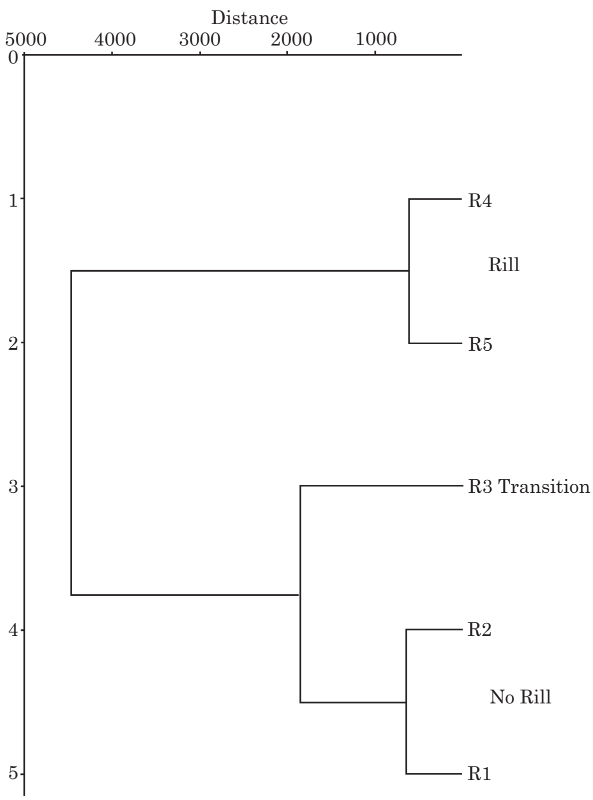

Figure 4. Hydraulic conditions throughout the experimental period, from RUN1 to RUN5 (Cophenetic correlation coefficient = 0. 905).

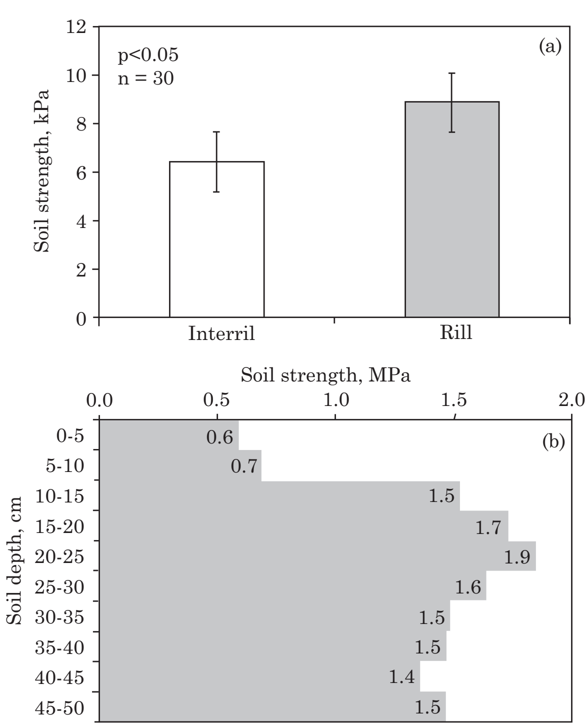

Figure 5. Soil strength discontinuity (compacted layer): a) the topsoil level measurement (Torvane test); and b) depth measurement (impact penetrometer).

The conventional tillage system generates soil anisotropy in the deeper layers (Figure 6) (e.g., soil strength, bulk density, and infiltration). While the topsoil was affected by disturbances, a subsurface compacted layer was generated in the deeper soil layers because of the limits of the cultivation equipment.

Consequently, the compacted layer can induce several subprocesses, which can decrease topsoil strength against surface runoff and facilitate subsurface flow. These processes are well-documented in the literature, and only some of the most common processes have been mentioned here.

The main effects of a compacted layer on soil erosion include the following: a) a rise in the water table or development of a transient water table (Lin et al., 2008; Bertolino et al., 2010), b) an abrupt decrease in the vertical transport capacity of water between the layers (i.e., hydraulic discontinuity) (Hemmat et al., 2007; Lin et al., 2008; Bertolino et al., 2010), and c) saturation-excess runoff and preferential flow in the soil (Lin et al., 2008).

Rills formed in the clay soil with a compacted layer have a U-shaped (flat) bottom because of the homogeneous strength of the compacted layer (Figure 6). These rills are shallow and can easily be removed

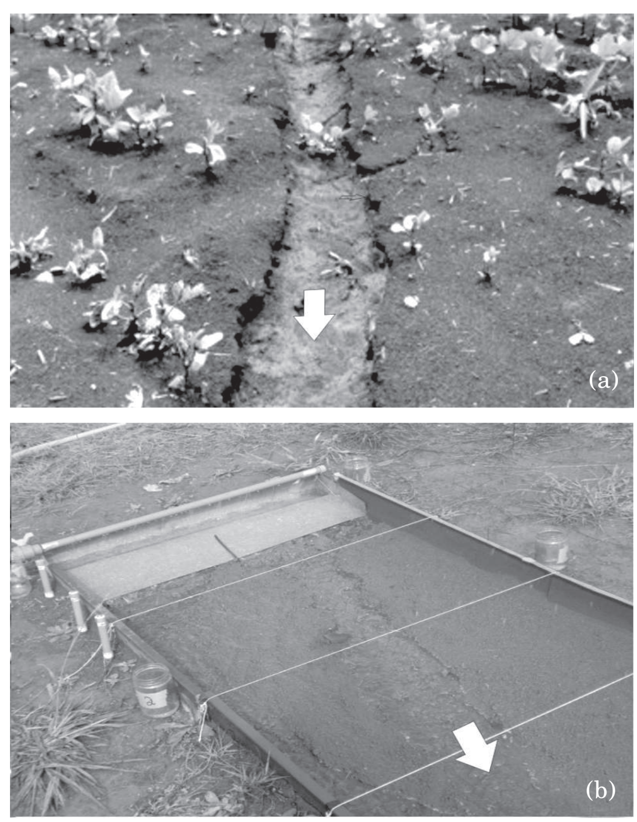

Figure 6. a) Rill formation related to a plow pan (field conditions); and b) rill deepening limited by the compacted layer (experimental conditions). The arrows indicate the compacted layer and flow direction.

between crops by tilling. However, during the rill development, large amounts of soil and contaminants can be transferred to the valley bottom through this channel. Therefore, a compacted layer results in more complex soil features and induces conditions for rill formation; which have not been widely considered in previous studies on soil erosion.

CONCLUSIONS

1. The hydraulic properties that induce sediment transport and rill formation are not the same, because of the resistance of the compacted layer; the hydraulic conditions leading to rill incision on the soil surface differed from the conditions inducing rill deepening.

2. The Reynolds number was the best hydraulic predictor for both processes. A rill incision occurs with a Reynolds number ≥5,000, a shear stress of ~11 (*Pa*) and a shear velocity of ≥0.1 m s^{-1}.

3. The compacted layer prevented rill deepening and avoided sediment detachment (detachment-limited).

4. The formed rills were shallow and could easily be removed by tillage between crops. However, during rill development, large amounts of soil and contaminants could also be transferred.

ACKNOWLEDGEMENTS

The author would like to thank João Augusto Coblinski, Fagner Dallaqua and Wolliver Anderson Dias for their support with the time-consuming fieldwork and laboratory tests.

LITERATURE CITED

AUZET, A.-V.; POESEN, J. & VALENTIN, C. Soil patterns as a key controlling factor of soil erosion by water. Catena, 46:85-87, 2002.

BERTOLINO, A.V.F.A.; FERNANDES, N.F.; MIRANDA, J.P.L.; SOUZA, A.P.; LOPES, M.R.S. & PALMIERI, F. Effects of plough pan development on surface hydrology and on soil physical properties in Southeastern Brazilian plateau. J. Hydrol., 393:94-104, 2010.

BLANCO, H. & LAL, R. Principles of soil conservation and management. London, Springer, 2010. 617p.

BOIX-FAYOS, C.; MARTÍNEZ-MENA, M.; ARNAU-ROSALÉN, E.; CALVO-CASES, A.; CASTILLO, V. & ALBALADEJO, J. Measuring soil erosion by field plots: Understanding the sources of variation. Earth Sci. Rev., 78:267-285, 2006.

BRYAN, R.B. Soil erodibility and processes of water erosion on hillslope. Geomorphology, 32:385-415, 2000.

BRYAN, R.B. Knickpoint evolution in rillwash. Catena, 17:111-132, 1990 (Supp. Bd.).

CHURCH, M. Observations and experiments. In: GREGORY, K.J. & GOUDIE, A.S., eds. The SAGE handbook of Geomorphology. London, SAGE Publications, 2011. p.121-141.

DUNKERLEY, D. Rain event properties in nature and in rainfall simulation experiments: a comparative review with recommendations for increasingly systematic study and reporting. Hydrol. Process., 22:4415-4435, 2008.

EVANS, R. The erosional impacts of grazing animals. Prog. Phys. Geogr., 22:251-268, 1998.

FARENHORST, A. & BRYAN, R.B. Particle size distribution of sediment transported by shallow flow. Catena, 25:47-62, 1995.

FOX, M.D. & BRYAN, R.B. The relationship of soil loss by interrill erosion to slope gradient. Catena, 38:211-222, 1999.

GOVERS, G.; GIMÉNEZ, R. & van OOST, K. Rill erosion: Exploring the relationship between experiments, modelling and field observations. Earth Sci. Rev., 84:87-102, 2007.

GREENE, R.S.B. & HAIRSINE, P.B. Elementary processes of soil–water interaction and thresholds in soil surface dynamics: a review. Earth Surf. Process. Landf., 29:1077-1091, 2004.

HAMZA, M.A. & ANDERSON, W.K. Soil compaction in cropping systems. Soil Till. Res., 82:121-145, 2005.

HEMMAT, A.; AHMADI, I. & MASOUMI, A. Water infiltration and clod size distribution as influenced by ploughshare type, soil water content and ploughing depth. Bio. Eng., 97:257-266, 2007.

HUGGINS, D.R. & REGANOLD, J.P. No-till system, a revolution in the preservation. Sci. Am. Braz., 75:57-63, 2008.

JULIEN, P.Y. Erosion and sedimentation. Cambridge, Cambridge University Press, 1998. 280p.

KNAPEN, A.; POESEN, J.; GOVERS, G.; GYSSELS, G. & NACHTERGAELE, J. Resistance of soils to concentrated flow erosion: A review. Earth Sci. Rev., 80:75-109, 2007.

LAL, R. Constraints to adopting no-till farming in developing countries. Soil Till. Res., 94:1-3, 2007.

LIN, H.; BROOKS, E.; MCDANIEL, P. & BOLL, J. Hydropedology and surface/subsurface runoff processes. In: ANDERSON, M.G., ed. Encyclopedia of hydrologic sciences. London, John Wiley & Sons, 2008. DOI: 10.1002/0470848944.hsa306.

MERZ, W. & BRYAN, R.B. Critical conditions for rill initiation on sandy loam Brunisols: laboratory and field experiments in southern Ontario, Canada. Geoderma, 57:357-385, 1993.

MORGAN, R.P.C. Soil erosion and conservation. Oxford, Blackwell, 2005. 304p.

ROCKWELL, D.L. Headcut erosive regimes influenced by groundwater on disturbed agricultural soils. J. Environ. Manage., 92:290-299, 2011.

RUYSSCHAERT, G.; POESEN, J.; VERSTRAETEN, G. & GOVERS, G. Soil loss due to crop harvesting: significance and determining factors. Prog. Phys. Geogr., 28:467-501, 2004.

SMITH, M.W.; COX, N.J. & BRACKEN, L.J. Applying flow resistance equations to overland flows. Prog. Phys. Geog., 31:363-387, 2007.

STOLF, R. Teoria e teste experimental de fórmulas de transformação dos dados de penetrômetro de impacto em resistência do solo. R. Bras. Ci. Solo, 15:229-35, 1991.

STROOSNIJDER, L. Measurement of erosion: Is it possible? Catena, 64:162-173, 2005.

THOMAZ, E.L. & VESTENA, L.R. Measurement of runoff and soil loss from two differently sized plots in a subtropical environment (Brazil). Earth Surf. Process. Landf., 37:363-373, 2012.

van OOST, K.; GOVERS, G.; DE ALBA, S. & QUINE, T.A. Tillage erosion: A review of controlling factors and implications for soil quality. Prog. Phys. Geogr., 30:443-466, 2006.